Evaluating the impact of using digital soil mapping products as input for spatializing a crop model: The case of drainage and maize yield simulated by STICS in the Berambadi catchment (India)

Philippe Lagacherie, Samuel Buis, Julie Constantin, Subramanian Dharumarajan, Laurent Ruiz, M. Sekhar

▶ To cite this version:

Philippe Lagacherie, Samuel Buis, Julie Constantin, Subramanian Dharumarajan, Laurent Ruiz, et al.. Evaluating the impact of using digital soil mapping products as input for spatializing a crop model: The case of drainage and maize yield simulated by STICS in the Berambadi catchment (India). Geoderma, 2022, 406, 10.1016/j.geoderma.2021.115503 . hal-03401773

Version of Record: https://www.sciencedirect.com/science/article/pii/S0016706121005838
Manuscript_4da7e2b36d191932165ce9aa9f26c3db

Evaluating the impact of using digital soil mapping products as input for spatializing a crop model: The case of drainage and maize yield simulated by STICS in the Berambadi Catchment (India)

Lagacherie[1], P.; Buis[2], S.; Constantin[3], J. ; Dharumarajan[4], S. ; Ruiz[5,6,8], L., Sekhar[7], M.

[1] LISAH, University Montpellier, IRD, INRAE, Montpellier SupAgro, 34060 Montpellier, France
[2] EMMAH, INRAE Avignon, France
[3] AGIR, INRAE, Toulouse, France
[4] ICAR-National Bureau of Soil Survey and Land Use Planning, Hebbal, Bangalore, 560024, India
[5] Géosciences Environnement Toulouse, Université Paul-Sabatier, IRD, CNRS, 31400 Toulouse, France; laurent.ruiz@inra.fr
[6] Indo-French Cell for Water Sciences, IRD, Indian Institute of Science, Bangalore 560012, India
[7] Indian Institute of Science, Civil Engineering Department, Bangalore 560012, India
[8] SAS, INRAE, Agrocampus Ouest, Rennes, France

Corresponding Author: P. Lagacherie : philippe.lagacherie@inrae.fr

Abstract

Digital Soil Mapping (DSM) can be an alternative data source for spatializing crop models over large areas. The objective of the paper was to evaluate the impact of DSM products and their uncertainties on a crop model's outputs in an 80 km^2 catchment in south India. We used a crop model called STICS and evaluated two essential soil functions: the biomass production (through simulated yield) and water regulation (via calculated drainage). The simulation was conducted at 217 sites using soil parameters obtained from a DSM approach using either Random Forest or Random Forest Kriging. We first analysed the individual STICS simulations, i.e., at two cropping seasons for 14 individual years, and then pooled the simulations across years, per site and crop season. The results show that i) DSM products outperformed a classical soil map in providing spatial estimates of STICS soil parameters, ii) although each soil parameters were estimated separately, the correlations between soil parameters were globally preserved, ii) Errors on STICS' yearly outputs induced by DSM estimations of soil parameters were globally low but were important for the few years with high impacts of soil variations, iii) The statistics of the STICS simulations across years were also affected by DSM errors with the same order of magnitude as the errors on soil inputs and iv) The impact of DSM errors was variable across the studied soil parameters. These results demonstrated that coupling DSM with a crop model could be a better alternative to the

classical Digital Soil Assessment techniques. As such, it will deserve more work in the future.

Keywords: Soil mapping, soil functions, digital soil assessment, crop model, machine learning, uncertainty analysis

1. Introduction

Spatializing a crop model consists of applying the model over an area much larger than those over which it was developed (Faivre et al, 2004). Various reviews (Hartkamp et al, 1999, Faivre et al, 2004, Ginaldi et al, 2019) provide examples of crop model spatialisation for a large range of purposes and at a large range of scales (from field to continental scales). Crop model spatialisation has been widely applied for assessing agricultural production and potentialities (e.g. Lal et al,1993), testing scenario about the impact of agricultural practices on water quality (e.g. Beaujouan et al, 2001), evaluating irrigation requirements (Sousa & Santos Pereira, 1999) or the impact of climate change on crop production (Wassenaar et al., 2000; Deryng et al., 2016). Several crop models were used in these spatialisations, the most common being DSSAT (Jones et al. 2003), APSIM (Keating et al. 2003), CropSyst (Stöcke et al. 2003), EPIC (Williams et al. 1989) and STICS (Brisson et al, 2003).

Among the different sources of uncertainty that may affect the spatialization of crop models, the estimation of the soil inputs is one of the most critical. Currently, the most common source of soil data used as input of crop models has been those provided by traditional choropleth soil maps (see e.g. table 1, Faivre et al., 2004). It is assumed that the best estimation of any soil property, and thus of soil inputs of the crop models, at an unvisited site covered by a soil map, is given by the soil mapping unit mean at all sites, often estimated by one so-called 'representative' soil profile. However, this assumption may generate a substantial uncertainty on soil inputs (Leenhardt et al., 1994a) that further propagates to the outputs of crop models (Leenhardt et al., 1994b). Alternative sources of soil data such as kriging of soil properties have been proposed (Faivre et al., 2004). However, to our knowledge, there has been no study in the literature using kriging of soil properties for spatializing a crop model beyond the field scale.

Digital Soil Mapping (DSM) can be an alternative to choropleth soil maps for providing the crop model soil inputs. DSM was developed as an alternative to conventional soil survey for mapping soil properties at limited costs (McBratney et al., 2003, Lagacherie et al., 2007). McBratney et al. (2003) proposed the equation S = f(s,c,o,r,p,a,n) for summarizing the general principle of DSM. According to this equation, a soil property (S) can be predicted by a spatial inference function (f) using, as input, the existing soil information (s), the spatial covariates that map the different factors of soil formation early defined by Jenny (1941) (c,o,r,p,a, standing for climate, organisms, relief, parent material and age respectively) and the geographical location (n) that can highlight any spatial trends missed by the other covariates. Although DSM is as much limited as conventional soil survey by the availability of the existing soil information, it has several important advantages over conventional soil survey: i) it exploits a large range of spatial data on landscape provided by the spatial data infrastructures, ii) it provides a local estimation of the uncertainty of predictions which allows making a realistic use of the outputs and iii) its outputs can be easily updated if new data are collected. DSM has moved rapidly to operationality thanks to the launch of the GlobalSoilMap projects (Arrouays et al, 2014), which enhanced the release of a number of GSM products providing soil property predictions at fine resolution at the national (e.g. Mulder et al., 2016, Adhikari et al., 2013), continental (e.g. Ballabio et al., 2019) and global (Hengl et al., 2007) scales.

Despite the rapid development of operational Digital Soil Mapping across the globe, it has rarely been envisaged yet as a possible source of soil inputs for spatializing mechanistic models (Tavares Wahren et al., 2016; van Tol et al., 2020) and, to our knowledge, has never been envisaged for spatializing crop models.

This paper aims to take the first step in filling this gap by evaluating the uncertainty of the outputs a crop model called STICS when it is simulated using soil inputs provided by a DSM approach compared to observed ones. The test was performed in an 80 km^2 catchment, located in south India. The study compared STICS outputs using observed soil parameters from a set of 217 soil profiles in the catchment, or by using the parameters estimated from DSM (Random Forest and Random Forest Kriging). We first analysed individual STICS simulations, i.e. at two crops seasons for 14 individual years and then pooled simulations across years, per site and crop season. We analysed two STICS outputs, which are essential for soil functions and ecosystem Services assessments at local sites (Adhikari & Hartemink, 2016): the biomass production (through yield) and the water regulation (through drainage).

2. Methods

2.1. Digital Soil Mapping

A classical Digital Soil Mapping approach was applied to map the soil properties required as inputs for the STICS soil crop model (denoted further the STICS soil inputs). This approach consisted in building a prediction function produced by a Random Forest (RF) (Breiman et al, 2001) or by a Regression Kriging algorithm (RK) (Hengl et al, 2004) with RF as regression algorithm (Vaysse et al., 2017), from a limited number of sites at which both the soil properties and the spatial data envisaged for to predicting soil properties are available. In the following, we give some details on the algorithms and on the validation approach.

2.1.1. Random Forest

Recent performance testing has found that the Random Forest was among the best models for predicting soil properties (Nussbaum et al., 2018), which confirmed a test performed on a wider range of machine learning applications (Caruana et al., 2006). We summarize hereafter the main principles of Random forest, using excerpts of Meinshausen (2006). More details are given on Random Forests in Breiman et al (2001) and Meinshausen (2006).

Let Y be a real-valued response variable and X be a covariate or predictor variable that is likely high-dimensional. A standard goal of statistical analysis is to infer the relationship between Y and X. Random Forests grow a large (>500) ensemble of trees using n independent observations (Y_i ,X_i), $i = 1, . . ., n$. Each tree grows via a recursive partitioning of the source set using one predictor variable X. At each step, the source set is split into two subsets following a test on the value of X. When Y is a quantitative variable, the selected test is the one that minimizes the within-subset variance of Y (Breiman et al., 1984). The recursive partitioning is limited by a stopping rule, and the subsets are produced by the last split being the leaves of the tree. The ensemble of trees is produced by using a random sample of the training data and a random subset of the predictor variables for each tree.

For the regression, the prediction $\hat{Y}_\theta(x)$of a single tree $\boldsymbol{\theta}$ of a Random Forest for a new data point x can be represented as the weighted average of the original observations Y_i, $i = 1, . . ., n$:

$$\hat{Y}_\theta(x) = \sum_{i=1}^{n} w_{\theta i}(x,\theta) Y_i \quad [4]$$

where $w_{\theta i}(x,\theta)$ is the weight vector given by a positive constant that is 1 if the observation

$Y_i$is part of the same leaf and 0 otherwise.

By using Random Forests, the prediction is the average prediction of *k*single trees that were constructed as described above.

$$\widehat{Y_T}(x) = \sum_{i=1}^{n} w_{Ti}(x) Y_i \qquad [5]$$

[5]

with $w_{Ti}(x) = k^{-1} \sum_{t=1}^{k} w_{\theta i}(x, \theta)$

The Random Forest Algorithm has three hyperparameters that must be fitted to obtain the best possible result, i) the number of observations drawn randomly for each tree, ii) the number of variables drawn randomly for each split and iii) the minimum number of samples that a node must contain. For the present study, the ranger package (Wright and Ziegler, 2017) was used for running the QRF algorithm in R environment.

2.1.2. Regression kriging with Random Forest

In Regression Kriging (RK), the estimated value at an unvisited site $\hat{Z}(s_0)$is given by summing the predicted value from regression $\widehat{m}(s_0)$and the residuals (i.e. the regression errors) interpolated by ordinary kriging $\hat{e}(s_0)$.

$$\hat{Z}(s_0) = \widehat{m}(s_0) + \hat{e}(s_0) \qquad [6]$$

In this application of RK, the trend function was obtained by calibrating a Random Forest (see above). The residuals were calculated at each observation point. An experimental variogram was then built from the residuals. If the visual inspection of the experimental variogram gave evidence of spatial structure, RK was applied for mapping the STICS soil input and the residuals were further interpolated onto the grid covering the study area by ordinary kriging. Otherwise, the prediction of RF was considered.

2.2. Crop modelling with STICS

STICS is a soil-plant simulation model, developed at INRA (France) in 1996 (Brisson et al, 2003). STICS can simulate the water, C and N balances of various types of crops, both annual and perennial, herbaceous and woody. STICS represents the plant-soil system dynamics depending on soil characteristics, climate and crop management. It simulates water, nitrogen and carbon balances at a daily time step within the soil-plant system. The soil is modelled using a tipping-bucket approach. The crop development is mainly driven by temperature, while crop biomass accumulation depends strongly on radiation interception by leaves. For water balance, the approach uses potential evapotranspiration (PET) and crop Leaf Area Index (LAI) to determine maximum evaporation and transpiration; the actual ones depending also on the soil water available for root uptake. When requirements are not met, water stress affects crop growth and yield depending on the severity and timing of the stresses. In this study, the impact of N stress on crop was not considered, therefore soil parameters that impact the model output are the depth of the soil layers, and for each layer the bulk density, water content at field capacity and at wilting point and rock fragment proportion. The 0-30cm surface layer is also characterized by its clay content that influences actual evaporation.

2.3. The case study

2.3.1. Berambadi catchment

The study was carried out in the Berambadi catchment located in the Deccan Plateau of South India (Figure 1), and spread over 84 km² (11°43'49" to 11°48'11" N Latitude and 76°32'31" to 76°36'14"). It belongs to the Kabini Critical Zone Observatory (CZO) (Sekhar et al., 2016), the Indian site of the SNO M-TROPICS (https://mtropics-fr.obs-mip.fr/), which is part of the OZCAR Research Infrastructure (Gaillardet et al. 2018; https://www.ozcar-ri.org). The elevation of the catchment ranges from 720 to 1362 m above mean sea level. The annual precipitation (2005-2018) is 993 mm, in which around 55% rainfall is received during the southwest monsoon (June to September) and 25% during the north-east monsoon (October to December). According to this rainfall distribution, agricultural practices are organized around two main cropping seasons: Kharif (May-August) and Rabi (September-December) (Sharma e al., 2018). Indeed, in the Berambadi catchment, the early start of the Kharif cropping season (before the onset of the SW monsoon) is possible because frequent convective storms occur in April and May. The average annual temperature is 22.6 °C. The soil moisture regime is ustic and soil temperature regime is isohyperthermic. The bedrock is granitic gneiss. Red soils (Alfisols) developed from Granitic parent material are found in uplands and hillslopes while Black soils (vertisols and its intergrades) are found in the valleys (Shivaprasad, 1998).

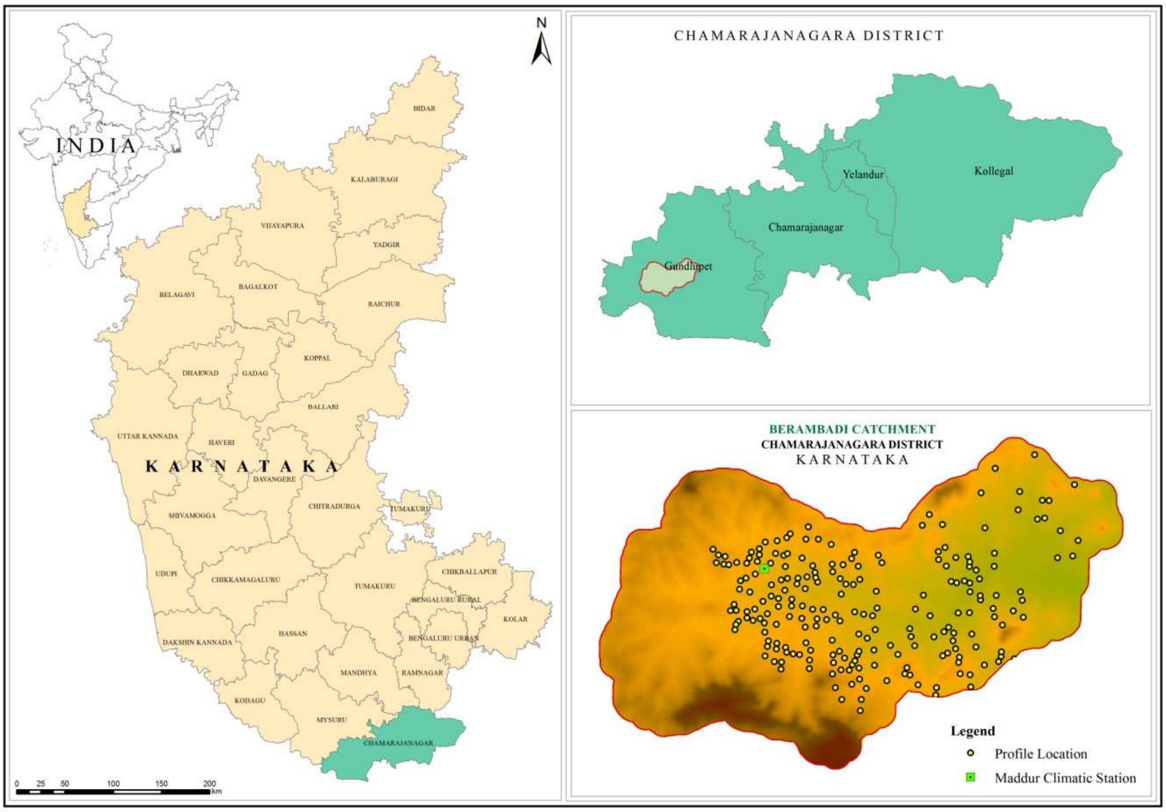

Figure 1. Study area, sampling locations (yellow dots) and climatic station (green dot)

2.3.2. Datasets

2.3.2.1. Soil data

We used soil observations from 217 soil profiles in the Berambadi catchment in sites selected for representing at best the soil variations (Figure 1, bottom right). A part of the sites was provided by the Sujala III project (http://watershed.kar.nic.in/SujalaIII_Doc.htm). The spatial sampling was completed by a soil survey carried out during April-May 2017 to fill the gaps. All the soil observations were performed following the protocol that is currently applied in India (NBSS&LUP staff, 2016). Each site was documented with the required soil properties for calculating the considered STICS soil inputs (see details below).

2.3.2.2. Soil Covariates

In Digital Soil Mapping, soil properties are predicted from a set of spatial data that are available over the whole study area, namely the soil covariates. A set of candidate soil covariates was provided as input of the DSM regression algorithm (here RF) (Table.1). A Digital elevation model (DEM) with 10 m resolution was obtained from Cartosat-1 and processed using ArcGIS10 data management toolbox. The first and secondary derivates of DEM like elevation, slope, aspect, curvatures (plan and profile) and topographic position index (TPI), Multi-resolution Index of Valley Bottom Flatness (MrVBF) and Multi-resolution Ridge Top Flatness (MrRTF) were derived by using Saga-GIS 2.3.1 version. Landform and soil order are derived from Legacy soil datasets of Chamrajnagar district (1: 50,000 scale). Normalized Difference Vegetation Index (NDVI) was extracted from satellite data for modelling. In addition, 10 bands of sentinel-2 data (Date of Acquisition : 24th April 2017) were used as covariates.

Source	name	Description
Cartosat DEM (10m)	elevation	Elevation
	Slope	Local Slope gradient
	Aspect	Local Slope Aspect
	Northeastness	Sin (Aspect + 45°)
	Northwestness	Cos(Aspect + 45°)
	Profile Curv	Curvature parallel to slope direction
	Plan Curfature	Curvature perpendicular to slope direction
	MRVBF	Multi Resolution Valley Bottom Flatness Index (Gallant & Dowling, 2003),
	MRRTF	Multi Resolution ridege Top Flatness Index (Gallant & Dowling, 2003),
	TPI	Topographical Position Index (mean difference of elevation with neighbouring pixels)
	TWI	Topographical Wetness Index (Sorensen et al, 2006) : Ln *a*/ tan *b,* with *a* the upstream area and *b* the slope gradient
Resourcesat-2 data (5.8m)	NDVI	Normalised Difference Vegetation index
Sentinel 2	Bands 2 to 8A and 11, 12	Different bands from Visible to NIR (10-20 m resolution)
1:50 000 Soil Map (KSRSAC, 2016)	landform	Landform
	Soil Order	USDA soil order

Table 1. Covariates used for DSM Model

2.3.2.3. Climate data

Daily values of rainfall, air humidity, wind velocity, maximum, minimum and mean air temperatures, precipitation and global radiation, that are required by STICS, were obtained from an automatic weather station (CIMEL, type ENERCO 407 AVKP from 2005 to 2015, and OTT type WS501 from 2016 to 2018) located in the study area (Figure 1).

2.4. The experiment

The two STICS outputs considered to assess the uncertainty when using the soil inputs provided by a DSM approach, crop yield and drainage, were selected for their importance in representing important soil functions (agricultural production and water regulation) and for their expected sensitivity to the soil inputs that could be mapped in the Berambadi catchment. Any other sources of uncertainty of STICS outputs, i.e. related with climate, agricultural practices and modelling errors, were removed from the experiment. In the following, we provide some details about the experiment designed accordingly.

2.4.1. The considered STICS soil parameters

The STICS soil layers were selected as those effectively observed by the soil surveyors in the field, namely, from top to bottom, the cultivated layer (A horizon), the horizon with pedogenic processes (B horizon) and the regolith till the occurrence of rock or paralithic contact (C horizon). For each layer, the following STICS soil inputs were considered: horizon thickness, clay content and albedo at the soil surface, bulk density, water content at Field Capacity (FC) and at Permanent wilting point (PWP).

Horizon thicknesses were directly derived from the soil profile observations. In the absence of laboratory measurements, clay contents were determined from the observed soil classes by taking the within-soil-class mean that were calculated from 20 soil profiles of the Berambadi catchment having particle size analysis. A similar approach was applied for estimating bulk density from existing datasets in the southern Deccan Plateau. Water contents at FC and PWP were determined from the observed textural classes using the following local pedotransfer function (PTF)s, established by using a dataset of 70 samples from the Berambadi catchment:

$$FC_{\text{fine earth}} = -4.7744+0.5403*\text{clay} \quad [7]$$

$$PWP_{\text{fine earth}} = -0.9054 +0.6265*\text{clay} \quad [8]$$

These pedotransfer functions provided FC and PWP as percentages of the fine earth, which may differ from the percentage of the whole soil layer for layers with non-null and variable rock fragment contents. In the STICS model, FC and PWP expressed in percentages of fine earth were converted into FC and PWP expressed in percentage of the whole soil layers, involving rock fragment contents (RFC) as follows:

$$FC_{soil\ layer} = FC_{fine\ earth} \times (100 - RFC)/100 \qquad [9]$$

$$PWP_{soil\ layer} = PWP_{fine\ earth} \times (100 - RFC)/100 \; [10]$$

The soil albedo was calculated from the Munsell soil color value recorded for the first described soil horizon, using the following PTF, developed by Post et al. (2000):

$$\text{Soil albedo } (0.3\text{-}2.8\ \mu m) = 0.069(\text{colour value}) - 0.114 \quad (R^2{=}0.93) \quad [11]$$

For all the remaining STICS parameters for which no data were available, we used the same values for all the 217 sites. STICS simulations were further designed accordingly to avoid any artefact related with this choice (see below). Finally, the 217 sets of STICS soil parameters derived from the observed soil properties were used to run STICS simulations, considered here as “ground truth”.

2.5. Spatial estimations of STICS soil parameters

The STICS soil parameters presented before were also estimated at the 217 sites with the DSM approach, from the set of soil covariates (section 3.2.2.) and using Random Forests (RF) or regression kriging (RK) (section 2.2.). For the STICS soil parameters derived from pedotransfer functions, the soil properties used as inputs of these functions were first estimated and then converted into STICS parameters by applying the corresponding PTFs. Consequently, the sets of estimated STICS parameters at the 217 studied sites were obtained from spatial estimations of the following properties of the three soil layers A, B and C: Soil layer thickness, Clay content, Rock Fragment, Field Capacity and Permanent Wilting point.

In order to obtain realistic results, the estimated STICS soil parameters at a given site had to be predicted from a DSM model (RF or RK) that was not calibrated from a dataset that included this site. To fulfil this requirement, a 10-fold cross-validation approach was repeated 20 times. At each of the 217 sites, the estimated values of the soil parameters were calculated as the mean of the 20 predicted values obtained when the site was not in the set of sites used for calibrating the DSM model.

2.6. STICS scenario simulations

The selected cropping system scenario was maize monoculture over the two main cropping seasons observed in the catchment, namely Kharif (from May to August, comprising early rains from convective storms followed by the South-West monsoon) and Rabi (from September to December, with rains from the North-East monsoon). We considered 14 climatic years available from the weather station, from 2005 to 2018. We assumed that considering the large inputs of N fertilizers in the catchment (Buvaneshwari et al., 2017), crops were sufficiently provided in nitrogen and we did not activate the module simulating N stress in the model. We selected Maize monoculture for all the simulations for three main reasons. First, itis very common in the Berambadi catchment and can be cultivated on all the local soil types. Second, as a rainfed crop, maize is expected to be very sensitive to water conditions that are in turn driven by the soil properties – and because of its deep rooting system, it is more sensitive to soil properties at depth than shallow-rooted crops. Last but not least, maize was among the few crops already calibrated in the STICS model for the same area (Sreelash et al., 2017).

According to the selected scenario, maize was assumed to be cultivated as follows: in Kharif, maize was sown on the 1st of May, and harvested on the 23rd of August. In Rabi, maize was sown on the 1st of September and harvested on the 19th of December. The simulations were initialized with soils at field capacity on the 1st of January of the first year, then were run continuously over the 14 years to better consider the effect of inter-annual variability of climate on soil water status and its impacts on crop production.

We considered 3038 (i.e. 14 years x 217 sites) couples of STICS outputs consisting of yield (t/ha) and drainage (mm). Furthermore, STICS outputs across years were summarized at each of the 217 sites by computing mean values, standard deviations, 25%, and 75% quartiles.

All these STICS outputs were computed twice, i.e from the observed STICS soil parameters (the ground truth) and from the estimated STICS soil parameters (see section 2.5.)

2.7. Evaluation protocol

The spatial estimations of the soil properties used to derive STICS soil parameter estimations (see section 2.5) and the STICS outputs (see section 2.6.) were compared to the same values obtained from observed soil properties using classical statistical indicators: Mean error (ME) or bias, Root Mean Square Error (RMSE) and the Mean Square Error Skill Score (SS_{MSE}, Nussbaum et al., 2018). When positive, SS_{MSE} expresses the percentage of explained variance by the predictive model. The definitions of these statistical indicators are provided below:

$$ME = \frac{\sum_i^n (P_i - O_i)}{n} \qquad (12)$$

$$RMSE = \sqrt{\frac{\sum_i^n (P_i - O_i)^2}{n}} \qquad (13)$$

$$SS_{mse} = \frac{\sum_i^n (P_i - O_i)^2}{\sum_1^n (O_i - \bar{O})^2} = \frac{RMSE^2}{Variance(O)} \qquad (14)$$

With *O* the observed value and *P* the predicted value

Besides this classical evaluation method, we also evaluated the DSM models for their ability to conserve the relationships between the parameters that were used together in the STICS simulations. Indeed, predicting separately each STICS soil parameters conveyed the risk of producing “pedo-chimeras” (e.g. a horizon with PWP greater than FC) that could have hampered the simulation results. The predicted correlations between STICS soil inputs were then evaluated by comparing them with the observed ones for each couple of parameters.

3. Results

3.1. STICS soil parameters

3.1.1. Observed soil data

Basic statistics of the STICS soil parameters as estimated from observations or from their pedotransfer function inputs are presented in Table. 2. The most variable soil properties across the Berambadi catchment (CV > 90%) were the rock fragment contents of B and C horizons, the thickness of the C horizons and the soil albedo. The least variable soil properties (CV < 30%) were the thickness of A horizons and the Field capacity of B and C horizons. The variations of the STICS soil parameters that were directly observed on the soil profiles (horizon thicknesses, rock fragment contents) were globally higher than those of the STICS soil parameters derived from the pedotransfer functions (Clay, FC, PWP).

Table 2. Summary statistics of STICS soil parameters

Soil properties	Layer	Min	Max	Mean	Stdev	CV (%)
Clay content (%)	A	13.4	49.4	27.3	13.3	48.7

Soil albedo	A	0.04	0.30	0.14	0.05	100.0
Thickness (cm)	A	6.0	43.0	17.8	5.0	28.1
	B	8.0	240.0	87.0	59.0	67.8
	C	0	140.0	28.0	27.0	96.4
Water at field capacity (%vol)	A	11.4	32.4	19.6	7.7	39.3
	B	11.4	32.4	21.9	5.8	26.5
	C	11.4	32.4	19.7	4.7	23.9
Water at wilting point (%vol)	A	3.8	19.3	9.8	5.7	58.2
	B	3.8	19.3	11.6	4.8	41.4
	C	3.8	19.3	9.9	3.5	35.4
Rock fragment (%)	A	0.0	50.0	18.4	10.9	59.2
	B	0.0	80.0	19.6	20.6	105.1
	C	0.0	80.0	21.1	22.8	108.1

Table 3. Performance of digital soil mapping approach and conventional soil mapping approach (between parenthesis) in prediction of different soil inputs. RK and QRF mean regression Kriging and Random Forest Respectively.

Soil properties	**Layer**	Model	SS_{MSE}	RMSE	Bias
Clay content (%)	A	RK	0.36 (0.18)	10 (12)	-0.03
Soil albedo	A	RK	0.26 (0.1)	0.04 (0.05)	0.0002
Thickness (cm)	A	RK	0.06 (0.1)	4 (4.65)	-0.01
	B	RK	0.40 (0.08)	45 (57)	-0.03
	C	RK	0 (0.04)	28.5 (26)	-0.07
Water at field capacity (%vol)	A	QRF	0.37 (0.16)	6.1 (7.3)	-0.01
	B	QRF	0.33 (0.06)	4.8 (6.1)	-0.12
	C	QRF	0.0 (0.08)	4.8 (11.7)	-0.79
Water at wilting point (%vol)	A	QRF	0.36 (0.17)	4.5 (5.6)	0.03
	B	QRF	0.36 (0.09)	3.8 (4.7)	0.03
	C	QRF	0 (0.07)	3.6 (6.3)	-0.55
Rock fragment (%)	A	RK	0.37 (0.13)	9 (10)	-0.004
	B	RK	0.35 (0.19)	16 (19)	-0.01
	C	RK	0.41(0.25)	17 (20)	-0.002

3.1.2. Estimated soil data by DSM

Random forest and Regression Kriging were applied to build prediction functions for all STICS soil parameters. Their evaluations over the 217 sites with soil observation using a ten-fold cross validation repeated 20 times (section 2.5.) allowed to select, for each STICS soil parameters, the best function. Regression Kriging model was selected for 8 out of the 14 mapped STICS soil parameters. For such parameters, the spatial interpolation of spatially structured residuals after RF predictions improved the results.

Most of the STICS soil parameters were predicted with negligible biases and moderate accuracy (between 33% and 41% of explained variance for 69 % of STICS outputs). The worst predictions (percentage of explained variance < 2%) were obtained for hydric properties of layer C and for the thickness of layer A. It is worth noting that these parameters also had the lowest standard deviations. The predictions of soil albedo had intermediate performances (26% of explained variance). Nevertheless, for all soil parameters, the comparisons with the R^2 and RMSE values obtained when using the mean values per soil mapping unit (digits between parenthesis in table 3) showed clearly that the DSM predictions clearly outperformed the soil map ones.

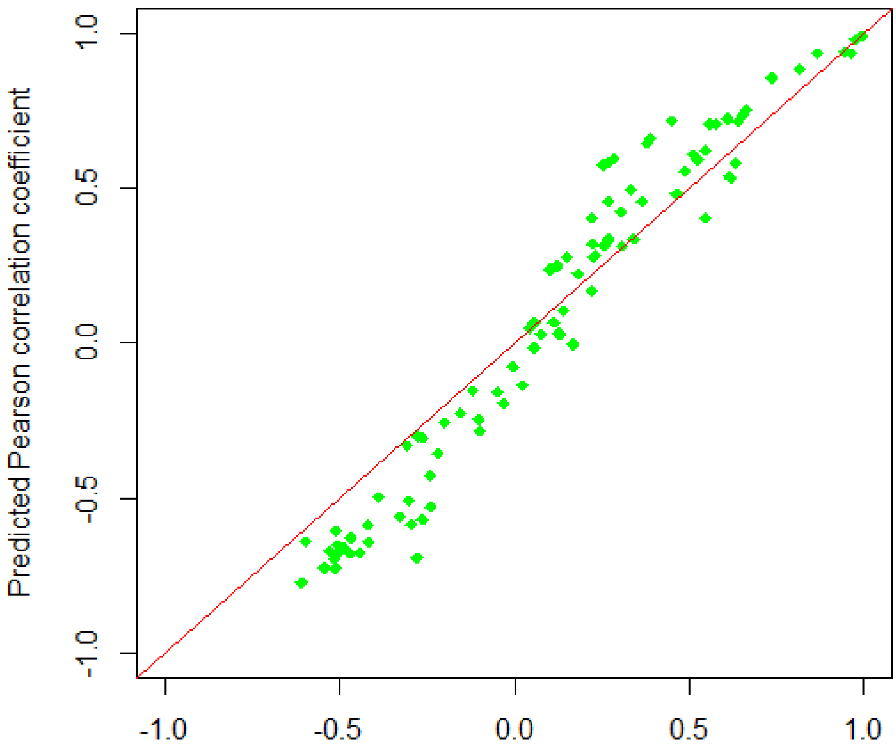

Figure 2. Observed correlation coefficient vs predicted correlation coefficient for each couple of predicted parameters

The comparisons between observed and predicted correlations between STICS soil inputs revealed an overall agreement (Figure 2). This means that, although the soil properties were predicted separately by different DSM models, the holistic vision of soils at each site was preserved without creating “pedo-chimeras” having unrealistic associations of soil property values.

3.2. STICS output statistics

We first analysed the STICS outputs obtained from observed soil inputs. Overall, the global impact of soil variations on the simulated results was weak to moderate depending on the output variables and seasons (figure 3). As expected, the impact of soil variability on yield was strongly correlated with the impact of soil variation on water stress (figures S1 and S2, supplementary materials). The mean over years of the standard deviations due to soil variations varied from about 2.5% to 10% of the global mean. However, results plotted per year (figure 4) show that this impact was extremely variable depending on the year. It was very low for yield in Kharif 2018 (standard deviation of 0.004 t ha^{-1}) whereas it was very high in Rabi 2017 (standard deviation of more than 0.8 t ha^{-1}). This impact was very low for drainage in Kharif 2011 (standard deviation of about 1 mm), whereas it was very high in Kharif 2007 (standard deviation of more than 25 mm in Kharif 2007). This means that, for some years, the levels of yield and drainage largely depended on the soil characteristics. Characterizing the years for which soil properties had a larger impact was not straightforward: while there was a clear relationship between the water balance and the mean and median values of yield and drainage (figure 4), it was not the case with their standard deviation (reflecting the impact of variations in soil properties). The effect of soil properties depended on complex intra-seasonal dynamics simulated by the model, as illustrated for the years 2005 and 2011 - (Figure S3, supplementary materials), which, despite similar seasonal water budgets, displayed contrasted impacts of soil properties on crop yield and drainage.

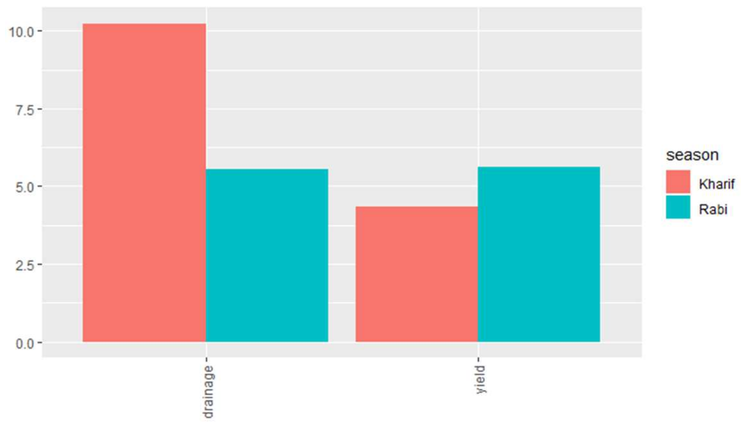

Figure 3. Mean of standard deviations over all years of simulation divided by the global mean (in %) for the different simulated variables.

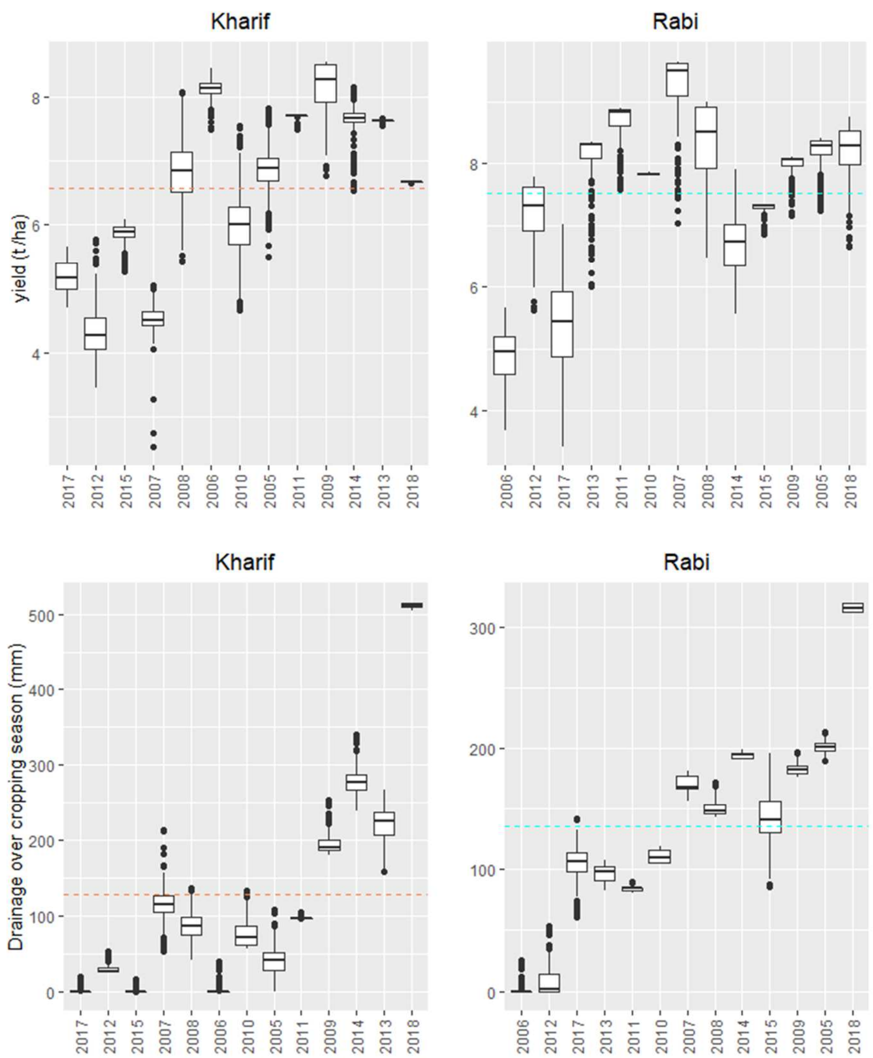

Figure 4. Variations with respect to soil inputs of simulated yield (above) and drainage over the growing season (below), per years, ordered from lowest to highest water availability, calculated as: Soil Water Content at sowing + (Rainfall – PET) over the growing season.

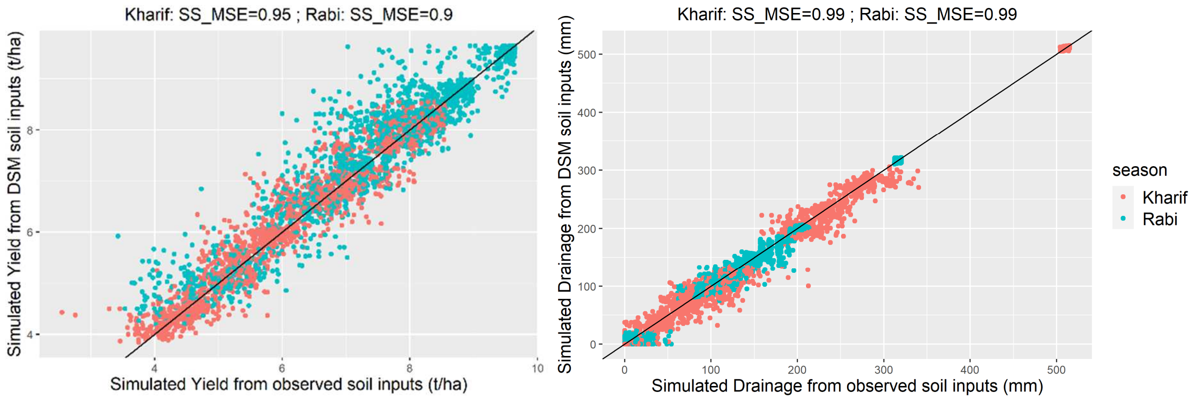

Figure 5. Simulated variables obtained from DSM soil inputs versus simulated variables obtained from observed soils. SS_MSE stands for Mean Square Error Skill Score (eq. 15).

3.3. DSM error impacts on STICS outputs

Errors induced by DSM estimations of STICS soil inputs were globally low with respect to the variations of the simulated variables (see R² and relative RMSE and biases given in % in figure 5). However, some of the yields simulated by STICS were far from the ones obtained with observed soil parameters.

To analyse this in more details, Figure 6 shows the impact of soil parameters variations (i.e. standard deviations per year of simulated results obtained on observed soils) on the simulation errors (RMSE per years). The RMSE was directly linked with the standard deviations of the simulated reference: the higher the impact of the soil, the higher the impact of soil parameters errors. For the years with the lowest soil impacts (left parts of the graph), the DSM errors on STICS outputs were close to their standard deviations, which means that DSM did not provide any insight on their spatial variation. However, beyond a given threshold of variation, the DSM errors were lower than standard deviations which means that the variations of STICS outputs related with the soil parameters were partially captured by DSM estimations as soon as they became important.

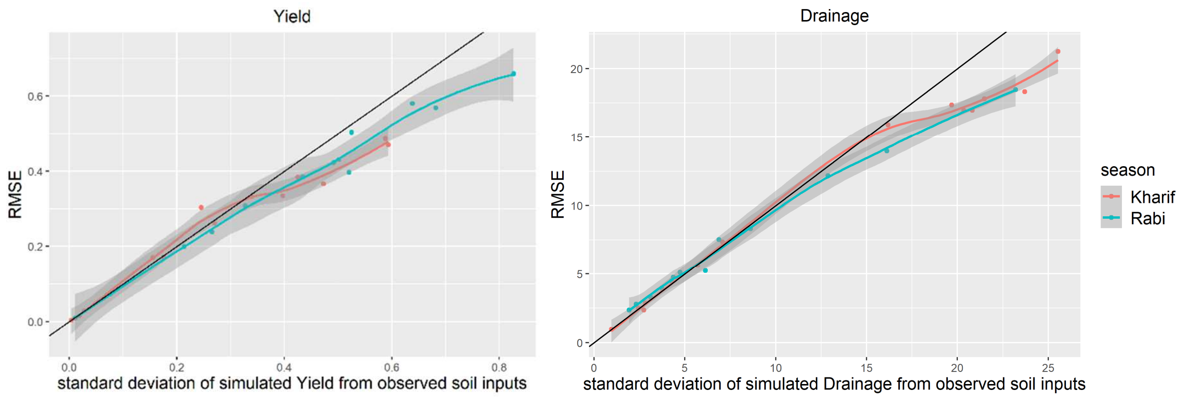

Figure 6. RMSE per year VS standard deviation of results obtained on observed soil per year. Left : yield (T/ha), right: drainage (mm)

3.4. Input-output errors correlations

We performed correlation analysis between residuals of STICS soil parameters and STICS outputs, to identify the soil parameters for which errors have the larger impact on the error of STICS outputs. Clay content on layers B and C and rock fragments were added to the analysis, although they were not direct STICS soil parameters, because they were involved in the PTF used for calculating FC and PWP, and thus were expected to strongly impact the STICS outputs values (see 4.1.).

The correlations between the residuals of STICS parameters and the STICS outputs were highly variable (Table 4). The water retention properties errors (water content at field capacity and wilting point) exhibited greater correlations than rock fragment errors and horizon depths errors, for all STICS outputs and the horizons. The errors on the B horizons parameters were the most correlated with STICS outputs, whatever the seasons and the outputs, with the noticeable exception of the rock fragment that exhibited a better correlation in the A horizon than in the B one. It is also apparent that the errors on drainage during the Rabi season were less correlated with STICS soil inputs than the other STICS outputs.

Table 4. Correlations between absolute errors on STICS outputs for different seasons and absolute errors on soil STICS inputs

Soil properties	Layer	Kharif		Rabi	
		Yield	Drainage	Yield	Drainage
Clay content (%)	A	0.38**	-0.53**	0.53**	0.06
Thickness (cm)	A	0.12	-0.11	0.09	-0.09
	B	0.37**	-0.40**	0.36**	-0.20**
	C	0.06	-0.03	-0.01	-0.07

Water at field capacity (%vol)	A	0.39**	-0.53**	0.54**	-0.04
	B	0.68**	-0.72**	0.73**	-0.44**
	C	0.40**	-0.39**	0.40**	-0.28**
Water at wilting point (%vol)	A	0.38**	-0.53**	0.53**	0.06
	B	0.58**	-0.63**	0.64**	-0.35**
	C	0.41**	-0.40**	0.41**	-0.29**
Rock fragment (%)	A	-0.21**	0.25**	-0.23**	0.00
	B	-0.11	0.10	-0.08	0.06
	C	-0.04	0.05	-0.07	0.01
Soil albedo	A	-0.12	0.20**	-0.22**	0.03

3.5. DSM error impacts on pooled STICS outputs per sites

The two STICS outputs were aggregated to provide their observed *vs* simulated distributions across the simulation period for each of the 217 sites. Different statistical indicators were used to describe these distributions outputs: mean, variance, 25% quartile and 75% quartile. Because of their contrasted climatic conditions, the results obtained for the two cropping seasons – Kharif and Rabi – were considered separately.

Figures 8 and 9 show contrasted results across seasons, STICS outputs, and statistical indicators with a limited range of R^2 (from 0.05 to 0.40) similar to those obtained for STICS soil parameters (Table 3). The scatterplots clearly show that the overall variability across sites was underestimated when the DSM estimated soil parameters were used instead of the observed ones. The lower values of all statistical parameters for yield were particularly underestimated showing that DSM did not simulate soils as limiting as to the observed ones (Figure 7). Conversely, the statistical parameters of drainage estimations were generally overestimated (Figure 8)

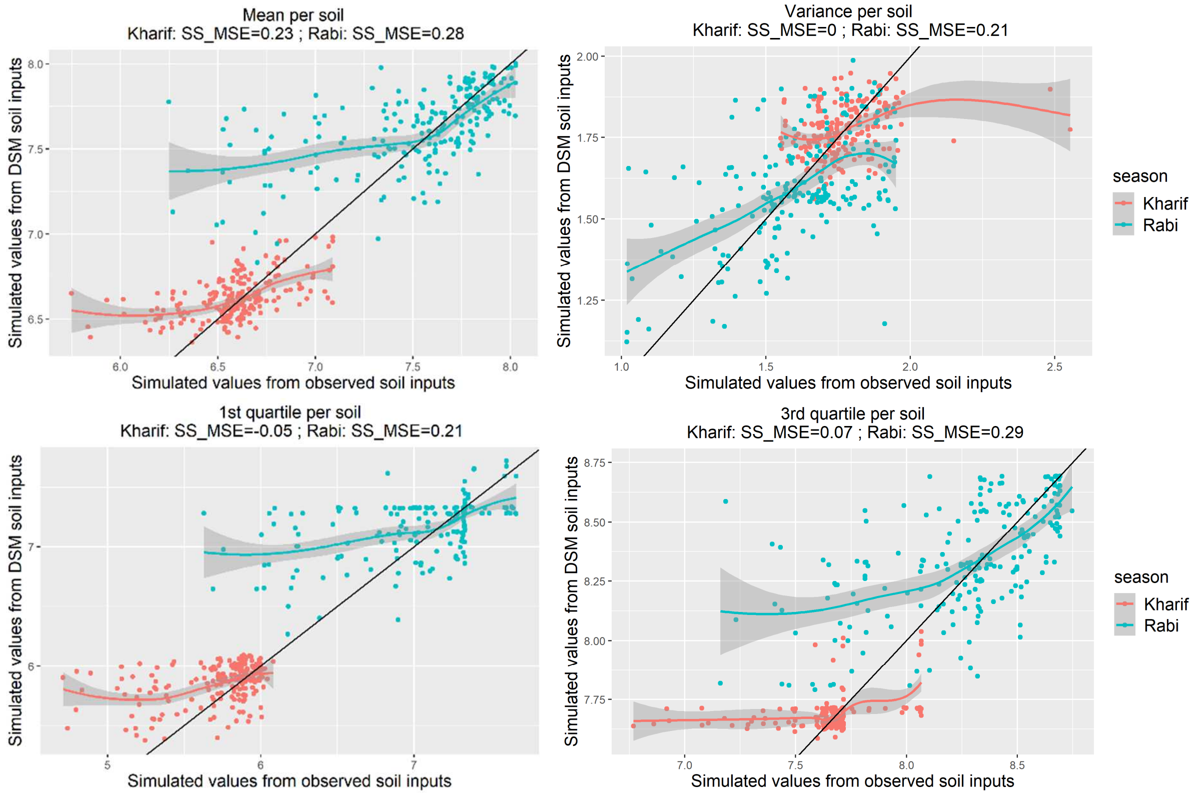

Figure 7. Mean, variance, 1st and 3rd quartile computed per soil, i.e. over years, of YIELD values simulated from DSM soil inputs VS equivalent but computed on values simulated from observed soils. SS_MSE stands for Mean Square Error Skill Score (eq. 15).

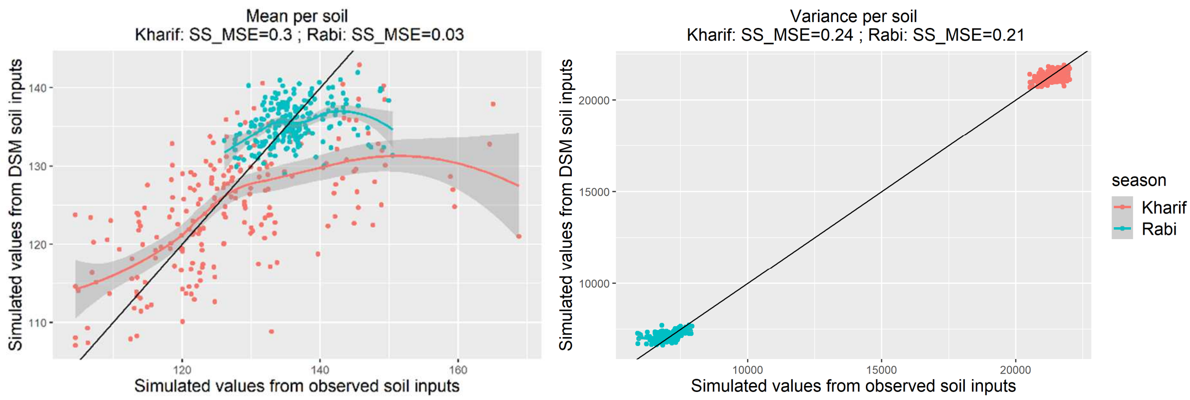

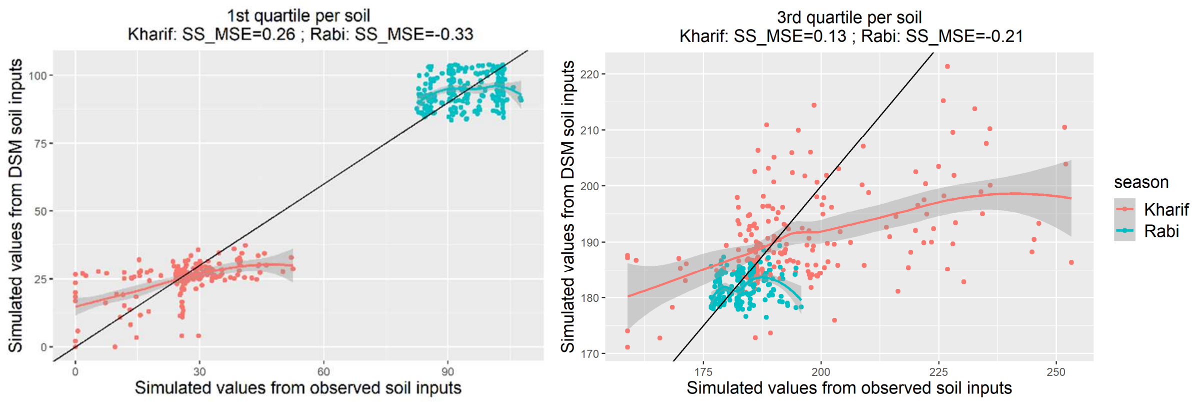

Figure 8. Mean, variance, 1st and 3rd quartile computed per soil, i.e. over years, of drainage values simulated from DSM soil inputs VS equivalent but computed on values simulated from observed soils. SS_MSE stands for Mean Square Error Skill Score (eq. 15).

All the statistical indicators of yield were better predicted in Rabi seasons than in Kharif season. Drainage showed opposite results with better performances for predicting statistical indicators in Kharif season than in Rabi seasons, with, here again, the noticeable exception of variance that did not exhibit significant differences between seasons. Mean and variance were generally better predicted than quartiles, which confirmed that DSM could not generate STICS parameters corresponding to extreme soil properties.

4. Discussion

4.1. Limiting factors of DSM performances

The present model captured only a part of the spatial variability for most of the soil properties. These results were not unexpected when looking at the DSM literature. For example, De Carvalho Jr et al. (2014) and Nussbaum et al. (2018) obtained SS_{MSE} values between 0 and 0.37 and between 0.08 and 0.28 respectively for particle size and rock fragment content predictions over Brasilian and Swiss areas of comparable extents and spatial densities of soil observations.

For all soil properties, the mapping errors were first due to the important sources of uncertainties that could affect the soil observations.

- Most of the observations were deduced from field determinations, without quantitative soil analysis, which induced uncertainty.
- The observations were affected by the variations of soil properties that can be observed at the profile scale, and that could be imperfectly described by a single value for a given soil property.

- the sampling of soil observations was too sparse to capture the part of the soil variations that occur at short distances. Indeed, as shown by several authors (Somarathna et al., 2017, Wadoux et al., 2018, Lagacherie et al., 2020), the spatial density of soil observations strongly impacts the performances of the DSM models.
- the presence of residuals after random forest analysis that justified the use of RK showed that the covariables used for explaining the variability of the soil input data were also not sufficient. New soil covariates should be added to capture the variability of soil properties better.

Finally, it should be noticed that these performances were measured for a prediction of soil properties at a point level, which is rarely required by end-users. Spatial aggregation of such predictions at larger spatial supports that make sense for user's decision, (e.g. fields) would dramatically decrease such error (Bishop et al., 2015; Vaysse et al., 2017).

Although the DSM estimations of soil parameters had important errors, it must be noticed that all these DSM estimations largely outperformed the spatial estimations of STICS soil parameters obtained from the existing soil map of the Berambadi (table 3). Furthermore, despite performing separate estimations of individual soil parameters and soil layers, we observed that the correlations between soil properties and layers were correctly predicted (Figure 2), which prevented from predicting pedo-chimera. This leads to prefer Digital Soil Mapping products to classical soil maps as sources of soil parameters for spatialising soil models.

4.2. Impacts of soil properties on STICS outputs.

Our experiment showed that the overall impact on yearly STICS outputs of soil variations in the Berambadi catchment was low (Figure 5). This result can be explained by the fact that, on one hand, the soils of the Berambadi catchment were quite deep (about 130 cm when including layer C, see table 2), and, on the other hand, because maize is a relatively deep-rooted crop, both factors buffering the soil-related variability in STICS output under ordinary climate conditions observed in the study area. Using a shallow-rooted crop in our simulations would have probably increased the impact of soil properties of the shallow horizons but it would have reduced even more the impact of deeper ones.

Interestingly, for few simulation years, soil variations had a greater impact on STICS results (Figure 4). These impacts of soils on crop yields could be significant enough to dramatically impact farmers' livelihood, considering the socio-economic vulnerability of farming systems in semi-arid regions of India (Singh et al., 2019). Moreover, we saw that such situations were linked with the complex dynamics of rain distribution and crop needs within the season, particularly the occurrence of drought periods early in the cropping season. Indeed, such situations might become more frequent in the future, as current projections for the Indian monsoon indicates increasing variability in monsoon rainfall and more frequent and severe drought spells (e.g. Sharmila et al., 2015)

This suggests that, in our case study, while crop models do not necessarily require an accurate representation of the distribution of soil properties for predicting the variations of yield and drainage across years, such information could become crucial for assessing the resilience of cropping systems in a changing climate.

4.3. Impact of DSM produced soil parameters errors

Our results showed that the spatialisation errors on the STICS soil parameters had an overall low impact on STICS simulation errors (figure 5) because of the low overall impact of soil variations on STICS outputs. However, a few simulations were strongly impacted by soil variations (see above), which in turn induced, for these situations, stronger impacts of DSM errors on the STICS outputs (figure 6). These impacts propagated to the statistical indicators that describe the behaviour of the sites across years (figure 7). It is interesting to note that the errors obtained on these statistical indicators were of the same order of magnitude as the spatialisation errors of soil parameters by DSM (table 3), showing neither smoothing nor amplifications of these spatialisation errors. Although the impact of soil estimations on crop model outputs have already been measured when using classical choropleth soil maps (Leenhardt et al., 1994b; Constantin et al., 2019; Hoffmann et al., 2016), to our knowledge, this was not been done yet when using DSM products. The level of error obtained with DSM being comparable to many DSM applications described in the literature (see 5.1.), this study can be considered a first reference for the use of crop modelling from DSM products. However, more studies will be necessary to get a complete picture of the interest and limitation of this new source of soil data.

Yet, this study only addressed a part of such errors. First, only perennial morphological and physical soil properties were addressed. The chemical soil properties that are also STICS soil inputs (i.e. pH, organic nitrogen) need to be considered in future studies. Furthermore, Permanent Wilting Point (PWP) and Field Capacity (FC) were not directly measured in the field but estimated from pedotransfer functions (PTF). The errors associated with these functions were not considered in this testing since the "observed" values of STICS outputs were produced from inputs that used also these functions. However, it has been shown (Roman-Dobarco et al., 2019) that the impact of PTF errors on the mapping of Soil Available Water Capacity was much lower than the mapping errors and thus could be neglected in most situations.

4.4. Most impacting soil characteristics

For the years for which soil variations matter (see the previous section), the same soil parameter errors affected STICS outputs differently at different seasons (Table 4). Correlation analysis also revealed that some STICS soil parameters errors affected the STICS outputs more than others. In some cases, these differences can be easily explained. For example, the predominant impact of the parameter related to the layer B on STICS parameter errors is probably because it represents the main part of the soil (87 cm against 18 and 28 cm for layer A and C, respectively), and the main source of water for root uptake across the cropping season. As the STICS model simulates a progressive increase of rooting depth across the vegetative phase of the crop, it was also expected that the parameters of horizon B related to the water holding capacity (FC and WP) would have had more impact on STICS outputs than its thickness. However, other differences are more difficult to interpret, such as the absence of impact of soils parameters on drainage for the Rabi season or the significant impact of rock fragments on both drainage and yield for horizon A but not for horizon B.
Overall, these results suggest that the impact of errors associated with simulated soil characteristics on the studied outputs, as modelled by STICS, is particularly complex. Sensitivity analysis methods may help in better understanding these impacts (Varella et al., 2010). Estimating relevant sensitivity indices would require considering the multivariate distributional properties of these errors and, in particular, the potentially complex dependency structure between them. This is still a challenge in the sensitivity analysis (Razavi et al, 2021) beyond the scope of this study.

4.5. Coupling DSM and crop models

Our study constitutes the first step in spatializing soil models using Digital Soil Mapping. Maps of statistical parameters of STICS output could be provided to users by using as STICS inputs the predicted parameters obtained by the DSM algorithms at the nodes of a regular grid covering the study area. Such maps would constitute an interesting alternative to the current maps of production functions of the soil that were derived from static combinations of soil properties (Kidd et al. 2015, Harms et al., 2015). Indeed, using a crop model to characterize such soil function would allow modulating soil assessment according to the spatial variations of other factors than soil, e.g. climate and agricultural practices (Ellili Bargaoui et al, 2021).

Apart from providing better soil parameter estimations than the ones provided by classical soil maps, DSM has the advantage of producing ex-ante estimations of the uncertainty of the soil property estimations (Heuvelink, 2014). Following error propagation techniques, such estimations could be propagated through STICS simulations (Vaysse et al; 2017). This would allow identifying the critical locations where the soil data are insufficient to estimate the required STICS soil parameters.

5. Conclusions

A first experiment of spatializing a crop model (STICS) using Digital Soil mapping was carried out in the Berambadi Catchment (India). The main lessons of this experiment are the following:

- Digital Soil mapping outperformed soil maps for spatializing STICS soil parameters while preserving correlation between soil parameters.
- Although the impact of DSM estimated soil parameters errors on yearly STICS outputs were on average low, some particular years exhibited strong differences between STICS outputs derived from observed vs DSM estimated soil parameters. The statistics of STICS simulations across years at each site giving a view of the crop production potential were also sensitive to DSM mapping errors
- The impact of DSM errors was variable across the involved soil parameters. Whereas some differences of impact could be easily explained, others would need a more thorough sensitivity analysis.
- Coupling DSM with a crop model represents an interesting alternative to the classical Digital Soil Assessment techniques. As such, it will deserve more work in the future.

6. Acknowledgments

The study was funded by the project ATCHA ANR-16-CE03-0006, and the Environmental Research Observatory M-TROPICS (https://mtropics.obs-mip.fr/), itself supported by the University of Toulouse, IRD and CNRS-INSU. We thank the SUJALA III project (Karnataka Watershed Development Department and World Bank) for their support. We also thank the farmers of the Berambadi catchment, for their kindness and support.

7. References

Adhikari, K., Greve, M.B., Bocher, P.K., Malone, B., Minasny, B., McBratney, A.B., Greve, M., 2013. High-Resolution 3-D Mapping of Soil Texture in Denmark. Soil Sci. Soc. Am. J. 860–876.

Adhikari, K., Hartemink, A.E., 2016. Linking soils to ecosystem services - A global review. Geoderma 262, 101–111.

Arrouays, D., Grundy, M.G., Hartemink, A.E., Hempel, J.W., Heuvelink, G.B.M., Hong, S.Y., Lagacherie, P., Lelyk, G., McBratney, A.B., McKenzie, N.J., Mendonca-Santos, M.D., Minasny, B., Montanarella, L., Odeh, I.O.A., Sanchez, P.A., Thompson, J.A., Zhang, G.-L., 2014. GlobalSoilMap. Toward a Fine-Resolution Global Grid of Soil Properties, Advances in Agronomy.125.

Ballabio, C., Lugato, E., Fernández-ugalde, O., Orgiazzi, A., Jones, A., Borrelli, P., Montanarella, L., Panagos, P., 2019. Mapping LUCAS topsoil chemical properties at European scale using Gaussian process regression. Geoderma 355, 113912.

Beaujouan V., Durand P., Ruiz L., Modelling the effect of the spatial distribution of agricultural practices on nitrogen fluxes in rural catchments, Ecol. Model. 137 (2001) 93–105.

Bishop, T.F.A., Horta, A., Karunaratne, S.B., 2015. Validation of digital soil maps at different spatial supports. Geoderma 241–242, 238–249.

Breiman, L., 2001. Random Forests. Mach. Learn. 45, 5–32.

Breiman, L., Friedman, J., Stone, C.J., Olshen, R.A., 1984. Classification and regression trees. CRC press.

Brisson,N., Gary,C.. Justes,E., Roche,R., Mary,B., Ripoche,D. Zimmer, D., Sierra,J., Bertuzzi,P., Burger, Bussiere,F., Cabidoche,Y.M., Cellier,P., Debaeke, P., Gaudillere,J.P., Henault, C., Maraux, F., Seguin, B., Sinoquet,H., 2003. An overview of the crop model STICS. European Journal of Agronomy, 2003, 18 (3-4), 309-332.

Buvaneshwari S, Riotte J, Sekhar M, Mohan Kumar MS, Sharma AK, Duprey JL, Audry S, Giriraj PR, Yerabham P, Moger H, Durand P, Braun JJ and Ruiz L (2017). Groundwater resource vulnerability and spatial variability of nitrate contamination: insights from high density tubewell monitoring in a hard rock aquifer. Science of the Total Environment, 579, 838-847. http://dx.doi.org/10.1016/j.scitotenv.2016.11.017

Caruana, R., Niculescu-Mizil, A., 2006. An empirical comparison of supervised learning algorithms. Proc. 23rd Int. Conf. Mach. Learn. - ICML '06 161–168.

Carvalho-Jr (de), W., Lagacherie, P., Da-Silva-Chagas, C., Calderano-Filho, B., Bhering, S.B., 2014. A regional-scale assessment of digital mapping of soil attributes in a tropical hillslope environment. Geoderma 232–234, 479–486.

Constantin, J., Raynal, H., Casellas, E., Hoffmann, H., Bindi, M., Doro, L., Eckersten, H., Gaiser, T., Grosz, B., Haas, E., Kersebaum, K.-C., Klatt, S., Kuhnert, M., Lewan, E., Maharjan, G.R., Moriondo, M., Nendel, C., Roggero, P.P., Specka, X., Trombi, G., Villa, A., Wang, E., Weihermüller, L., Yeluripati, J., Zhao, Z., Ewert, F., Bergez, J.-E., 2019. Management and spatial resolution effects on yield and water balance at regional scale in crop models. Agric. For. Meteorol. 275, 184–195. https://doi.org/10.1016/j.agrformet.2019.05.013

Deryng D, Elliott J, Folberth C, Müller Pugh CTAM, Boote KJ, Conway D, Ruane AC, Gerten ,D, Jones JW, Khabarov N, Olin S, Schaphoff S, Schmid E, Yang H, Rosenzweig C (2016) Regional disparities in the beneficial effects of rising CO2 concentrations on crop water pro- ductivity. Nat Clim Chang 6(8):786–790

Ellili-bargaoui, Y., Walter, C., Lemercier, B., Michot, D., 2021. Assessment of six soil ecosystem services by coupling simulation modelling and field measurement of soil properties. Ecol. Indic. 121, 107211.

Faivre, R., Leenhardt, D., Voltz, M., Benoit, M., Papy, F., Dedieu, G., Wallach, D., 2004. Spatialising crop models. agronomie 24, 205–217.

Gaillardet, J., Braud, I., Hankard, F., Anquetin, S., Bour, O., Dorfliger, N., ... & Zitouna, R., 2018. OZCAR: The French network of critical zone observatories. *Vadose Zone Journal*, *17*(1), 1-24.

Gallant, J.C., Dowling, T.I., 2003. A multiresolution index of valley bottom flatness for mapping depositional areas. Water Resour. Res. 39.

Ginaldi, F., Bajocco, S., Bregaglio, S., Cappelli, G., 2019. Spatializing crop model for sustainable agriculture, in: Farooq, M., Pisante, M. (Eds.), Innovations in Sustainable Agriculture. Springer Nature Switzerland, pp. 599–620.

Harms, B., Brough, D., Philip, S., Bartley, R., Clifford, D., Thomas, M., Willis, R., Gregory, L., 2015. Digital soil assessment for regional agricultural land evaluation. Global Food Security, Global Food Security 5, 25–36. https://doi.org/https://doi.org/10.1016/j.gfs.2015.04.001

Hartkamp A.D., White J.W., Hoogenboom G., Interfacing Geo-graphic Information Systems with Agronomic Modeling: AReview, Agron. J. 91 (1999) 761–772.

Hengl, T., Heuvelink, G.B.M., Stein, A., 2004. A generic frameword for spatial prediction of soil variables based on regression-kriging. Geoderma 120, 75–93.

Hengl, T., De Jesus, J.M., Heuvelink, G.B.M., Gonzalez, M.R., Kilibarda, M., Blagotić, A., Shangguan, W., Wright, M.N., Geng, X., Bauer-Marschallinger, B., Guevara, M.A., Vargas, R., MacMillan, R.A., Batjes, N.H., Leenaars, J.G.B., Ribeiro, E., Wheeler, I., Mantel, S., Kempen, B., 2017. SoilGrids250m: Global gridded soil information based on machine learning. PLoS One 12, 1–40.

Heuvelink, G.B.M., 2014. Uncertainty quantification of GlobalSoilMap products, in: Arrouays, D., McKenzie, N.J., Hempel, J.W., Richer de Forges, A., McBratney, A.B. (Eds.), GlobalSoilMap: Basis of the Global Spatial Soil Information System - Proceedings of the 1st GlobalSoilMap Conference2014. CRC press/Balkema, London, pp. 335–340.

Hoffmann, H., Enders, A., Siebert, S., Gaiser, T., Ewert, F., 2016. Climate and soil input data aggregation effects in crop models. Havard Database V3. https://doi.org/https://doi.org/10.7910/DVN/C0J5BB

Jenny, H., 1941. Factors of Soil Formation, A System of Quantitative Pedology. McGraw-Hill, New York.

Jones JW, Hoogenboom CH, Porter KJ, Boote WD, Batchelor LA, Hunt PWW, Singh U, Gijsman AJ, Ritchie JT (2003) The DSSAT cropping system model. Eur J Agron 18(3–4):235–265

Keating BA, Carberry PS, Hammer GL, Probert ME, Robertson MJ, Holzworth D, Huth NI, Hargreaves JNG, Meinke H, Hochman Z, McLean G, Verburg K, Snow V, Dimes JP, Silburn M, Wang E, Brown S, Bristow KL, Asseng S, Chapman S, McCown RL, Freebairn DM, Smith CJ (2003) An overview of APSIM, a model designed for farming systems simulation. Eur J Agron 18:267–288

Kidd, D., Webb, M., Malone, B., Minasny, B., Mcbratney, A., 2015. Geoderma Regional Digital soil assessment of agricultural suitability , versatility and capital in. GEODRS, GEODRS 6, 7–21. https://doi.org/10.1016/j.geodrs.2015.08.005

KSRSAC (2016), Karnataka GIS asset database, version 1, Karnataka State Remote Sensing Applications Centre, Dept. of IT, BT and S & T, Govt. of Karnataka

Lagacherie, P., McBratney, A.B., Voltz, M., 2007. Digital Soil Mapping: An Introductory perspective, ,. ed. Elsevier, Amsterdam.

Lagacherie, P., Arrouays, D., Bourennane, H., Gomez, C., Nkuba-kasanda, L., 2020. Analysing the impact of soil spatial sampling on the performances of Digital Soil Mapping models and their evaluation : A numerical experiment on Quantile Random Forest using clay contents obtained from Vis-NIR-SWIR hyperspectral imagery. Geoderma 375.

Lal H., Hoogenboom G., Calixte J.P., Jones J.W., Beinroth F.H., (1993) Using crop simulation models and GIS for regional productivity analysis, Trans. ASAE 36 (1993) 175–184

Leenhardt, D., Voltz, M., Bornand, M., Webster, R., Science, L. De, Viala, P., I, M.C., 1994a Evaluating soil maps for prediction of soil water properties. Eur. J. Soil Sci. 45, 293–301.

Leenhardt, D., Voltz, M., Bornand, M., 1994b. Propagation of the error of spatial prediction of soil properties in simulating crop evapotranspiration. Eur. J. Soil Sci. 45, 303–310.

McBratney, A.B., Mendonca-Santos, M.D., Minasny, B., 2003. On digital soil mapping. Geoderma 117, 3–52.

Meinshausen, N., 2006. Quantile Regression Forests. J. Mach. Learn. Res. 7, 983–999.

Mulder, V.L., Lacoste, M., Richer-de-Forges, A.C., Arrouays, D., 2016. GlobalSoilMap France: High-resolution spatial modelling the soils of France up to two meter depth. Sci. Total Environ. 573, 1352–1369.

NBSS&LUP staff, 2016. Field Guide for Land Resources Inventory, Sujala III project Karnataka, NBSS Publ. ICAR-NBSSLUP, Bangalore 154p.

Nussbaum, M., Spiess, K., Baltensweiler, A., Grob, U., Keller, A., Greiner, L., Schaepman, M.E., Papritz, A., 2018. Evaluation of digital soil mapping approaches with large sets of environmental covariates. Soil 4, 1–22.

Razavi, S., Jakeman, A., Saltelli, A., Prieur, C., Iooss, B., Borgonovo, E., Plischke, E., Lo Piano, S., Iwanaga, T., Becker, W., Tarantola, S., Guillaume, J.H.A., Jakeman, J., Gupta, H., Melillo, N., Rabitti, G., Chabridon, V., Duan, Q., Sun, X., Smith, S., Sheikholeslami, R., Hosseini, N., Asadzadeh, M., Puy, A., Kucherenko, S., Maier, H.R., 2021. The Future of Sensitivity Analysis: An essential discipline for systems modeling and policy support. Environmental Modelling & Software 137, 104954.

Sekhar, M., Riotte, J., Ruiz, L., Jouquet, P., & Braun, J. J., 2016. Influences of climate and agriculture on water and biogeochemical cycles: Kabini critical zone observatory. In *Proc. IndianNatl. Sci. Acad,* 82(3), 833-846.

Sharma, A., Hubert-Moy, L., Buvaneshwari, S., Sekhar, M., Ruiz, L., Bandyopadhyay, S., & Corgne, S. (2018). Irrigation history estimation using multitemporal Landsat satellite Images: application to an intensive groundwater irrigated agricultural watershed in India. Remote Sensing, 10(6), 893. http://dx.doi.org/10.3390/rs10060893

Sharmila, S., Joseph, S., Sahai, A. K., Abhilash, S., & Chattopadhyay, R. (2015). Future projection of Indian summer monsoon variability under climate change scenario: An assessment from CMIP5 climate models. Global and Planetary Change, 124, 62-78.

Shivaprasad, C. R., Reddy, R. S., Sehgal, J., Velayutham. M., 1998. Soils of Karnataka for optimizing land use. NBSS&LUP publication No.47b, Nagpur.

Singh, C., Solomon, D., Bendapudi, R., Kuchimanchi, B., Iyer, S., & Bazaz, A. (2019). What shapes vulnerability and risk management in semi-arid India? Moving towards an agenda of sustainable adaptation. Environmental Development, 30, 35-50.

Sørensen, R.; Zinko, U.; Seibert, J. (2006). "On the calculation of the topographic wetness index: evaluation of different methods based on field observations". *Hydrology and Earth System Sciences*. 10 (1): 101–112.

Somarathna, P.D.S.N., Minasny, B., Malone, B.P., 2017. More Data or a Better Model? Figuring what Matters Most for the Spatial Prediction of Soil Carbon. Soil Sci. Soc. Am. J. 81, 1413–1426.

Sousa V., Santos Pereira L., 1999. Regional analysis of irrigation water requirements using kriging. Application to potato crop (Solanumtuberosum L.) at Tras-os-Montes, Agric. Water Manage. 40 .21–233.

Sreelash, K., Buis, S., Sekhar, M., Ruiz, L., Tomer, S. K., &Guerif, M. (2017). Estimation of available water capacity components of two-layered soils using crop model inversion: Effect of crop type and water regime. Journal of Hydrology, 546, 166-178.

Stöckle CO, Donatelli M, Nelson R (2003) CropSyst, a cropping systems simulation model. Eur J Agron 18(3):289–307

Tavares, F., Julich, S., Pedro, J., Gonzalez-pelayo, O., Hawtree, D., Feger, K., Jacob, J., 2016. Combining digital soil mapping and hydrological modeling in a data scarce watershed in north-central Portugal. Geoderma 264, 350–362.

van Tol, J. Van, Zijl, G. Van, Julich, S., 2020. Importance of Detailed Soil Information for Hydrological Modelling in an urbanized environment. hydrology 1–15.

Varella, H., Guérif, M., Buis, S. (2010). Global sensitivity analysis measures the quality of parameter estimation: the case of soil parameters and a crop model. *Environmental Modelling & Software*, *25*(3), 310-319.

Vaysse, K., Lagacherie, P., 2017. Using quantile regression forest to estimate uncertainty of digital soil mapping products. Geoderma 291, 55–64.

Vaysse, K., Heuvelink, G.B.M., Lagacherie, P., 2017. Spatial aggregation of soil property predictions in support of local land management. Soil Use Manag. 33.

Wadoux, A.M.J., Brus, D.J., Heuvelink, G.B.M., 2019. Sampling design optimization for soil mapping with random forest. Geoderma 355.

Wassenaar, T., Lagacherie, P., Legros, J.P., Rounsevell, M.D.A., 1999. Modelling wheat yield responses to soil and climate variability at the regional scale. Clim. Res. 11.

Williams JR, Jones CA, Kiniry JR, Spanel DA , 1989. The EPIC crop growth model. Trans Am Soc Agric Eng 32:497–511

Wright, M.N., Ziegler, A., 2017. ranger : A Fast Implementation of Random Forests for High Dimensional Data in C ++ and R. J. Stat. Softw. 77.